Journal of Catalysis 361 (2018) 407–413

Contents lists available at ScienceDirect

Journal of Catalysis

journal homepage: www.elsevier.com/locate/jcat

Isolation of an acetylide-Cu^{I}_{3}-tris(triazolylmethyl)amine complex active in the CuAAC reaction

Haoqing Chen [a], Chirine Soubra-Ghaoui [b], Zhiling Zhu [a], Siheng Li [a], Thomas A. Albright [a], Chengzhi Cai [a,*]

[a] Department of Chemistry, University of Houston, 3585 Cullen Blvd, Houston, TX 77204-5003, USA
[b] Department of Chemistry & Physics, University of St. Thomas, 3800 Montrose, Houston, TX 77006-4626, USA

ARTICLE INFO

Article history:
Received 6 October 2017
Revised 21 February 2018
Accepted 26 February 2018

Keywords:
Click chemistry
CuAAC reaction
Intermediate
X-rays
Mechanism

ABSTRACT

The CuAAC click reaction is greatly accelerated by tris(triazolylmethyl)amine ligands (**TL**). Using mass spectrometry, we found a trinuclear **TL**–Cu^{I}_{3}–acetylide complex formed in the reaction. Under catalytic conditions, the trinuclear complex is more active than the proposed dinuclear complex, whereas in a single-turnover reaction, the dinuclear complex is more reactive. Here, this finding is rationalized by analysis of the first single-crystal X-ray structure of a trinuclear **TL**–Cu^{I}_{3}–acetylide complex and DFT calculation, revealing how **TL** stabilizes the trinuclear complex, which may accelerate the reaction by promoting coordination with an azide followed by dissociation of a Cu^{I} to form a more favorable dinuclear transition state.

1. Introduction

Cu^{I}-catalyzed azide–alkyne cycloaddition (CuAAC) [1,2] is one of the most important reactions in "click chemistry" for site-specific conjugation of diverse molecular building blocks. Its high efficiency, orthogonality, and simplicity have given it broad applications in bioconjugation, medicinal chemistry, and materials science [3–5].

The mechanism of the CuAAC reaction has been investigated both computationally [6–11] and experimentally [11–15]. The rate-determining step (RDS) in the CuAAC reaction was initially assigned to formation of the first N—C bond of the triazole ring, which requires the highest activation energy, based on computational studies [6–9]. Further investigations suggest that the RDS under catalytic conditions may vary depending on the solvent [15–17], ancillary ligands [18], alkyne and azide reagents [17,19–27], and possibly counterions [28]. For example, the calculated energy barrier for alkyne deprotonation is quite high in dichloromethane [16]. Consistently, the deprotonation step in one system was slower than the ring-closure step in dichloromethane as determined experimentally [15].

Another factor that contributes to the reaction rate is the structure of alkyne and azide. The employment of chelating azides [17,19–22] and electron-deficient alkynes [23–26] that stabilize the azide–Cu^{I}–acetylide ternary complex can greatly accelerate the CuAAC reaction. Iacobucci *et al.* reported the observation of a zide–copper–acetylide in the absence of PPh_3 ligand or in the presence of a nearby charge in the alkyne substrate in solution [14] and in the gas phase [11]. In the presence of the PPh_3 ligand, however, they only observed the copper triazolide product [11], indicating that the ligand not only stabilized the copper complex but also accelerated the reaction, and the cyclization step might no longer be the RDS. Recently, Seath *et al.* observed the shift of the RDS from acetylide formation to the azide ligation/migratory insertion event using benzimidazolyl alkyne [27]. Calculations also suggested a non-negligible energy barrier for the azide–Cu^{I}–acetylide ternary complex formation [7–10]. In the presence of strong coordinating ancillary ligands or solvents that inhibit the alkyne–Cu^{I} binding, the acetylide generation step turns to RDS again [18]. Although the RDS of CuAAC is influenced by many factors, activation of alkyne and azide by multiple Cu^{I} centers was generally proposed as the key factor influencing the reaction rate.

Efforts have been made to isolate the Cu^{I} acetylides in CuAAC reaction to shed light on the mechanism through study of the coordination structure. Although Cu^{I} acetylides have been extensively studied [29,30], the indiscriminate aggregation of Cu^{I} acetylides remains a major obstacle to preparing and isolating well-characterized multinuclear [C≡C—Cu^{I}_{n}] complexes. For the ancillary ligand-free and strong ligand-accelerated CuAAC reactions, several di-Cu^{I} acetylide complexes in the reaction have been isolated, all of which were stabilized by strong Cu^{I} ligands,

* Corresponding author.
E-mail address: cai@uh.edu (C. Cai).

https://doi.org/10.1016/j.jcat.2018.02.024
0021-9517/

e.g., N-heterocyclic carbenes (NHC) [13,31,32], cyclic(alkyl)(amino)-carbenes (CAAC) [15], pyridinyl ligands [33], or organophosphines [34]. Nonetheless, the multi-Cu^{I} acetylide complexes bearing weakly binding ligands, typically the tris(triazolylmethyl)amine ligands (**TL**), which are more reactive than the reported strong ligands, have not been isolated before due to their low stability in solution.

The **TL** ligands, such as tris[(1-benzyl-1*H*-1,2,3-triazol-4-yl) methyl]amine (**TBTA**) [35] and its derivatives, are some of the most widely used Cu^{I} ligands in the CuAAC reaction [5,18,36–38]. Indeed, the **TL** ligands showed the best accelerating effect in aqueous solutions among a library of tripodal amine ligands [39]. Despite their wide use, the mechanistic role of **TL** ligands remains poorly understood [18,19]. Using electrospray ionization mass spectrometry (ESI-MS), we recently identified a **TL**-stabilized tri-Cu^{I} acetylide intermediate in aqueous solutions [40]. Our kinetic data showed that the tri-Cu^{I} acetylide was less reactive than the di-Cu^{I} acetylide in a single-turnover model system using a **TL**–alkyne conjugate. However, under catalytic conditions, the trinuclear **TL**–Cu^{I}_3–acetylide complex contributed much more to the overall reaction rate than the dinuclear **TL**–Cu^{I}_2–acetylide complex [40]. In the absence of the **TL** ligand, these multi-Cu^{I} intermediates were undetectable and the reaction was much slower. To rationalize these results and shed light on the role of **TL** in the CuAAC reaction, structural information on the multinuclear **TL**–Cu^{I}–acetylide complex is highly desirable. Here, we report the first single-crystal X-ray structure of a trinuclear **TL**–Cu^{I}_3–acetylide complex and the density functional theory (DFT) calculation of the energy barriers of the reaction via the trinuclear vs. the dinuclear complexes.

2. Experimental

2.1. Materials and methods

Reagents and solvents were purchased from Sigma-Aldrich, VWR, or TCI America and used without further purification. LC-MS grade methanol and acetonitrile were purchased from VWR. The ultrapure water for all experiments was obtained from Milli-Q water purification systems. The single-crystal X-ray structure was obtained using a Bruker DUO platform diffractometer equipped with a 4 K CCD APEX II detector. Elemental analysis for copper was performed using an Agilent 725 ICP-OES instrument. Positive ion ESI-MS data were acquired using a Thermo Finnigan LCQ Deca XP ion trap mass spectrometer. Positive ion MALDI-TOF mass was recorded on an AB SCIEX 4800 MALDI TOF/TOF analyzer using α-cyano-4-hydroxycinnamic acid as a matrix. FT-IR was characterized using a Nicolet iS10 FT-IR spectrometer. NMR spectra were recorded on a JEOL ECX-400, ECA-500, or ECA-600 spectrometer.

2.2. Synthesis of complex 1

The synthesis of complex **1** was performed in a nitrogen glove box and all solvents were pre-degassed. To a stirred solution of **TATA** (Fig. 1, 20 mM in CH_2Cl_2, 1 mL) was added alkyne **2** (Fig. 1, 100 mM in MeOH, 200 μL), $Cu(MeCN)_4PF_6$ (30 mM in MeOH, 2 mL), and Milli-Q water (100 μL) under N_2. The solution was stirred for 6 h, transferred to a small beaker, and blow-dried with a flow of nitrogen. The pale yellow residue was redissolved in a mixed solvent of MeOH (1 mL) and CH_2Cl_2 (1 mL) (1:1 ratio) and then filtered into a 5 mL glass vial. The vial (without a cap) was placed inside a tightly capped 20 mL glass vial containing ether (5 mL) to allow slow diffusion of ether vapor into the complex solution. To reduce vibration and thermal fluctuation, the 20 mL vial was wrapped with cotton and placed in a beaker covered with aluminum foil to shield it from light. After a week of incubation at room temperature inside the nitrogen glove box, complex **1** was obtained as pale yellow needle crystals. The melting point of complex **1** was measured using the newly grown crystals, which were washed with methanol ×1 and ether ×1 and then dried in the glove box. The resulting pale yellow smaller crystals were moved out of the glove box and the melting point was measured in air. The crystals turned brown at 165 °C (decompose).

2.3. NMR spectroscopic analysis

In a nitrogen glove box, the newly grown crystals of complex **1** were washed with methanol ×1 and ether ×1 (the solvents were removed by pipettes) and dried for several minutes. The drying procedure resulted in the breaking down of the needle-shaped crystals into tiny pale yellow crystals, and solvent molecules in the crystal might be rapidly evaporated during the process [41,42]. The complex was then dissolved in 70% (99.8% D) CD_3OD and 30% (99.9% D) CD_2Cl_2. The solution was sealed in a screw-capped NMR tube and the ^{1}H, ^{1}H–^{1}H DQF-COSY, and ^{19}F NMR spectra were recorded at room temperature (see the Supplementary Data for the NMR spectra).

2.4. Single-crystal X-ray diffraction analysis

Newly grown single crystals of complex **1** were taken out from the mother liquor and immediately put under mineral oil without any washing and drying. A large single crystal was picked out and immediately frozen to −150 °C for single-crystal X-ray diffraction analysis. All measurements were made with a Bruker DUO platform diffractometer equipped with a 4 K CCD APEX II detector and an Incoatec 30 W Cu microsource with compact multilayer optics. A hemisphere of data (2713 frames at 4 cm detector distance) was collected using a narrow-frame algorithm with scan widths of 0.50° in ω and an exposure time of 40 s/frame at 123 K. The data were integrated using the Bruker SAINT program, with the intensities corrected for Lorentz factor, polarization, air absorption, and absorption due to variation in the path length through the detector faceplate. The data were scaled, and an absorption correction was applied using SAINT v7.60A. The structure was solved with SHELXT 2014 and refined with SHELXL 2014 using

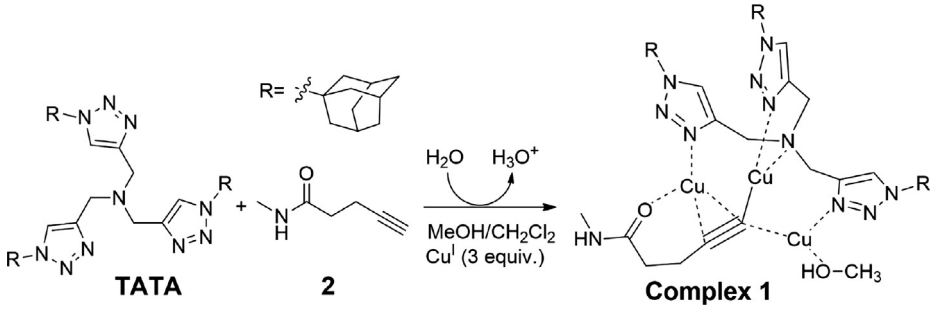

Fig. 1. Self-assembly of **TATA**, alkyne **2**, and Cu^{I} to form single crystals of **TATA**–Cu^{I}_3–acetylide (complex **1**) from MeOH/CH_2Cl_2/Et_2O.